Morphology and Properties of Low-Carbon Bainite

H. OHTANI, S. OKAGUCHI, Y. FUJISHIRO, and Y. OHMORI

Morphology of low-carbon bainite in commercial-grade high-tensile-strength steels in both isothermal transformation and continuous cooling transformation is lathlike ferrite elongated in the $\langle 111 \rangle_b$ direction. Based on carbide distribution, three types of bainites are classified: Type I, is carbide-free, Type II has fine carbide platelets lying between laths, and Type III has carbides parallel to a specific ferrite plane. At the initial stage of transformation, upper bainitic ferrite forms a subunit elongated in the $[\bar{1}01]_f$ which is nearly parallel to the $[111]_b$ direction with the cross section a parallelogram shape. Coalescence of the subunit yields the lathlike bainite with the $[\bar{1}01]_f$ growth direction and the habit plane between $(232)_f$ and $(111)_f$. Cementite particles precipitate on the sidewise growth tips of the Type II bainitic ferrite subunit. This results in the cementite platelet aligning parallel to a specific ferrite plane in the laths after coalescence. These morphologies of bainites are the same in various kinds of low-carbon high-strength steels. The lowest brittle-ductile transition temperature and the highest strength were obtained either by Type III bainite or bainite/martensite duplex structure because of the crack path limited by fine unit microstructure. It should also be noted that the tempered duplex structure has higher strength than the tempered martensite in the tempering temperature range between 200 °C and 500 °C. In the case of controlled rolling, the accelerated cooling afterward produces a complex structure comprised of ferrite, cementite, and martensite as well as BI-type bainite. Type I bainite in this structure is refined by controlled rolling and plays a very important role in improving the strength and toughness of low-carbon steels.

I. INTRODUCTION

THE morphology of upper bainite is very similar to that of lath martensite elongated in a $[\bar{1}01]_f$ direction with a habit plane between $(111)_f$ and $(232)_f$.[1–6] Although upper bainitic ferrite forms without partitioning the substitutional alloying elements, it contains much fewer carbon atoms than the austenite from which it forms. The carbide particles in upper bainite are exclusively cementite, and alloy carbides have never been recognized. These facts show the possibilities that the upper bainite may form *via* a displacive mechanism as far as the substitutional elements are concerned though it may accompany the diffusion of interstitial elements.[3,5,7–14]

The bainite of low-carbon steel always has lathlike ferrite. In this sense, all the bainites formed in low-carbon steels should be classified into upper bainite. But there exist three types of cementite morphologies:[3] Type I is carbide-free, Type II has the cementite particles in the shapes of layers between them,[15] and Type III has fine platelets lying parallel to a specific ferrite plane in the interior. The latter morphology of cementite is especially predominant in the bainite at relatively lower temperatures in the vicinity of *Ms* temperature and is often thought of as evidence of lower bainite,[16] as depicted in Table I.

The production of high-tensile-strength steel, on the other hand, is performed by a continuous cooling process such as quenching, moderate accelerated cooling, and normalizing. The microstructure, therefore, is composed of a mixture of various kinds of transformation products such as martensite, bainite, and ferrite. Above all, the bainite plays an important role in obtaining strength and toughness. For example, the toughness of the transformation products is not always monotonically dependent on cooling rate.[17] There is an optimum cooling rate for high toughness, and the microstructure to obtain the lowest brittle-ductile transition temperature was confirmed to be bainite/martensite duplex structure. This is probably due to the refinement of the effective grain size by the bainite formation prior to that of martensite. It is also reasonable that the bainite has tempering characteristics different from those of martensite because of its different cementite precipitation behavior.

In addition to the conventional heat treatment, the thermomechanical process, *i.e.*, the combination of controlled rolling and accelerated cooling, has been widely adopted. The microstructures of the materials produced by these processes become very difficult to identify because the microstructures are very fine and are comprised of various transformation products.

This paper will describe the microstructural aspects in some detail and will discuss the relationship between the morphology and properties of bainite in low-carbon high-strength steels.

II. EXPERIMENTAL PROCEDURES

A. *Materials*

Materials were prepared by vacuum induction melting and hot rolled in the laboratory. Commercially produced continuous cast slab and hot-rolled plate were also used. Chemical compositions appear in Table II.

H. OHTANI, General Manager of Tube and Pipe Department, S. OKAGUCHI, Research Engineer, and Y. OHMORI, Principal Research Manager, are with the Research and Development Division, Sumitomo Metal Industries, Ltd., Amagasaki 660, Japan. Y. FUJISHIRO, Assistant Manager, is with Osaka Steel Works, Sumitomo Metal Industries, Ltd., Osaka 554, Japan.

This paper is based on a presentation made in the symposium "International Conference on Bainite" presented at the 1988 World Materials Congress in Chicago, IL, on September 26 and 27, 1988, under the auspices of the ASM INTERNATIONAL Phase Transformations Committee and the TMS Ferrous Metallurgy Committee.

Table I. Morphology of Bainite in Isothermal Transformation

Phase	Criteria	
	Ferrite Morphology	Carbide Distribution
Ferrite	lathlike	acicular ferrite (carbide-free)
Upper bainite	BI BII BIII	lath interface
Lower bainite	platelike	within grain

B. *Transformation Study*

The specimens machined to 1- to 2-mm thick were austenitized at 1150 °C to 1200 °C and isothermally transformed for various times in molten salt or lead in the bainite transformation range between 750 °C and 400 °C. After holding, they were quenched into iced brine to decompose the untransformed austenite into martensite. For continuous cooling, dilatometric measurements by Formaster F and Thermecmaster (Fuji Electronic Industrial Co., Tokyo, Japan) were carried out. Optical and electron microscopy were also performed. The continuous-cooling-transformation (CCT) diagram and the isothermal transformation diagram were drawn based on these data.

C. *Examination of Mechanical Properties*

The specimens with thicknesses of 7 to 25 mm were heated at 900 °C to 1200 °C for 15 minutes and cooled at various cooling rates. Cooling rates were controlled by the selection of quenchants such as iced brine, water, oil, and air. Isothermal heat treatment was also carried out to produce a fully bainite structure. Both the as-transformed and the tempered specimens were used for tensile and V-notch Charpy impact tests. Fractured surfaces were examined by means of scanning electron microscopy (SEM).

The specimens produced by the accelerated cooling after the controlled rolling were prepared as follows. A 150-mm-thick slab heated at 1100 °C to 1150 °C was roughly rolled to 70 mm, then control rolled to 19 mm in the temperature range between 780 °C and 740 °C, and then air cooled or accelerated cooled at the cooling rates of 10 °C to 20 °C/s.

III. MORPHOLOGY OF BAINITE

A. *Isothermal Transformation*

The time-temperature-transformation (TTT) diagram of Cu-Ni-Cr-Mo steel determined by metallographic examination[3] is shown in Figure 1. At the temperature below 600 °C, the bainite transformation occurs. The bainitic ferrite has lathlike morphology. Above 500 °C, the transformation was not completed within the time examined, and the bainite is composed of bunches of ferrite lath with the untransformed austenite between them. Carbide could not be observed (Type I). Below 500 °C, the cementite layers were mainly formed at the ferrite lath interfaces by the decomposition of the carbon-enriched austenite, although a small amount of cementite platelet precipitated within ferrite grains aligned in a certain direction (Type III). The mode of cementite distribution looks very similar to lower bainite in high-carbon steels. Nevertheless, all these bainites of a low-carbon steel have the same $\sim\langle 111\rangle_b$ $(110)_b$ lathlike morphology. It seems reasonable to classify them as upper bainite, as the separation between upper and lower bainite is defined by ferrite morphology. The width of lath changed with isothermal transformation temperature:[19] 2 μm at 500 °C, 1 μm at 500 °C, and 0.2 μm at 425 °C, respectively.

Figure 2 shows the optical microstructures in high magnification of a Si-Mn steel which was transformed isothermally. The lathlike bainitic ferrite can be seen clearly. At the early stage of transformation, cementite particles were not observed between laths. After a long time holding isothermally at 550 °C, the coalescence of lath and the pearlite transformation of the austenite between them occur. The change of lath width with temperature is consistent with a former report.[19]

Transmission electron microscopy (TEM) for the partially transformed specimens revealed that an upper bainite lath consists of a number of small subunits similar to those observed within a massive structure.[9] An example of the subunits of Cr-Mo-B steel formed at 500 °C is shown in Figure 3. In this case, the growth direction of the bainite laths (also that of the subunit)[20] is normal to the micrograph (the $[11\bar{1}]_b$ direction in Figure 3. The subunit/austenite (martensite) interphase boundaries can clearly be seen in Figure 3(a). The selected area electron diffraction pattern in Figure 3(b) comprises two sets of net patterns, the one from the upper bainite subunits and the other from the martensite islands formed by the decomposition of the untransformed austenites between the subunits. The close examination of the subunit shown in Figure 4 demonstrates that the subunit/austenite

Table II. Chemical Compositions of Materials (Weight Percent)

Steel	C	Si	Mn	P	S	Cu	Ni	Cr	Mo	V	B	Nb	Ti	Sol. Al	N
A	0.12	0.30	0.83	0.004	0.005	0.30	1.11	0.53	0.49	0.03	—	—	—	0.031	—
B	0.22	0.24	0.83	0.008	0.012	0.30	1.05	0.54	0.51	0.02	—	—	—	0.029	—
C	0.20	0.30	0.97	0.010	0.005	—	—	1.37	0.59	—	0.0010	—	0.015	0.061	—
D	0.08	0.28	1.57	0.011	0.002	—	—	—	—	0.07	—	0.03	0.018	0.042	0.0038
E	0.02	0.16	1.85	0.005	0.004	—	—	—	—	—	0.0011	0.05	0.019	0.029	0.0035
F	0.03	0.37	1.70	0.005	0.004	—	—	—	—	—	0.0010	0.04	0.020	0.040	0.0020

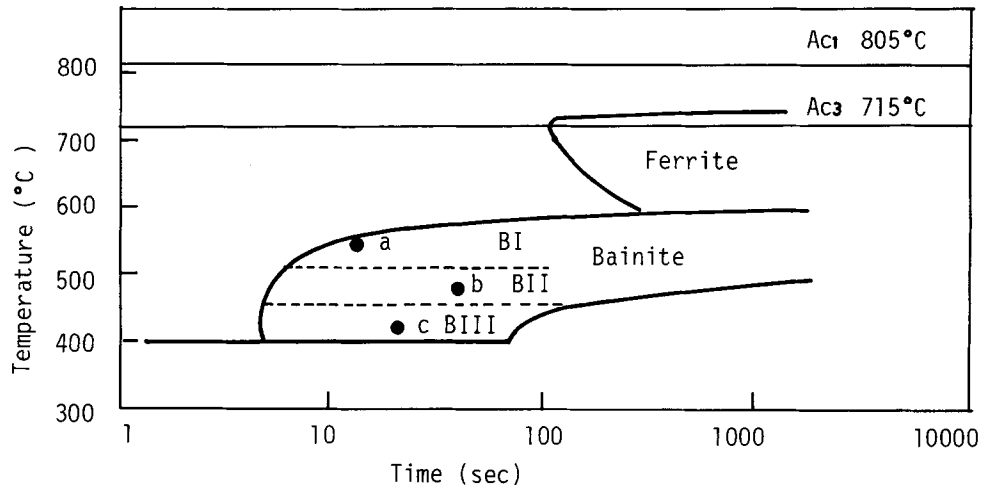

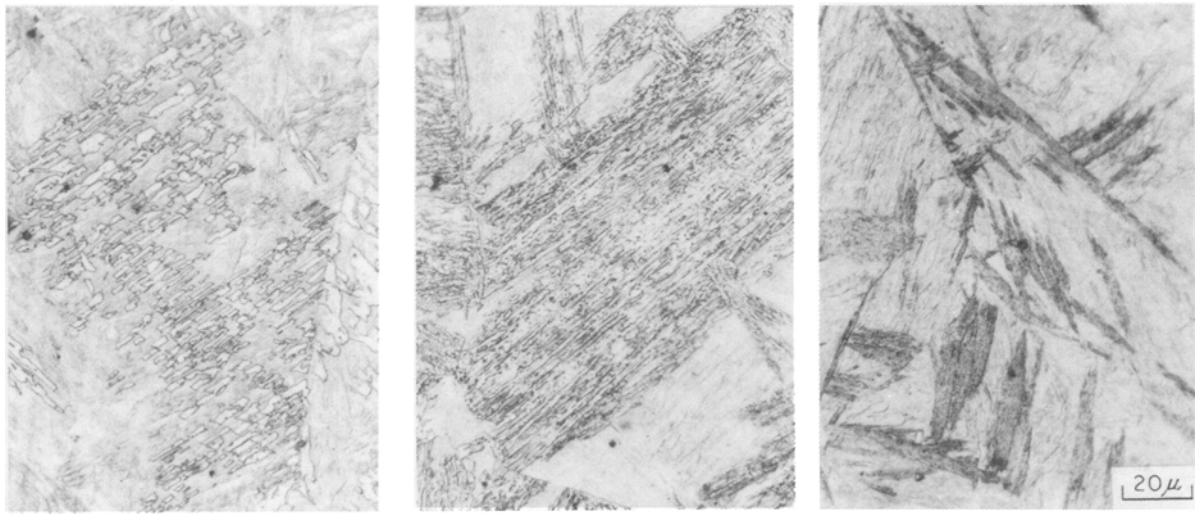

(a) BI (570°C, 15sec) (b) BII (475°C, 40sec) (c) BIII (400°C, 25sec)

interfaces consist of the ledges sharply edged in specific orientations. The stereographic analysis assuming that the Kurdjumov-Sachs relationships[21] hold between the prior austenite and these two transformation products provides a specific orientation of the parent austenite, as can be seen in Figure 5. The orientation relationships expected between the upper bainite subunits and the austenite and between the martensites and the austenite are

$$\begin{cases}(011)_b /\!/ (111)_f \\ (111)_b /\!/ (10\bar{1})_f \\ (2\bar{1}1)_b /\!/ (1\bar{2}1)_f\end{cases} \quad \text{and} \quad \begin{cases}(011)_m /\!/ (111)_f \\ (111)_m /\!/ (\bar{1}10)_f \\ (\bar{2}1\bar{1})_m /\!/ (11\bar{2})_f\end{cases}$$

respectively, where "f," "b," and "m" denote the austenite, the bainite, and the martensite. The surface trace normals for the bainitic ferrite subunits, *i.e.*, the one normal to the lath habit planes and the other normal to the lath edges, lie in the regions between the $(121)_f$ and the $(111)_f$ and between the $(101)_f$ and the $(212)_f$, respectively. Such trace analyses carried out for various orientations were always consistent with the results described above.

Figure 6 demonstrates that cementite platelets precipitate on these bainitic ferrite subunit untransformed austenite (martensite) interphase boundaries. It is also of interest that the traces of lath edges and cementite platelets are almost parallel to those of the transformation twins in the martensite layers between the bainite laths. The coalescence of the subunits results in the upper bainite laths, as shown in Figure 7(a). It should, however, be pointed out that the cementite layers have not precipitated between the laths in this structure and that they form mostly at the final stage of transformation. The cementite platelets in the lath interior, on the other hand, align on the planes of a specific orientation but in a slightly wavy fashion. The selected area electron diffraction pattern shown in Figure 7(b) indicates that the cementite platelets are related to the ferrite as in the previous studies[22,23] and can be expressed as

$$(010)_c /\!/ (11\bar{1})_b$$
$$(103)_c /\!/ (011)_b$$

The trace analysis for the bainite laths and the cementite platelets in the interior, by fixing the ferrite/cementite orientation relationship to a specific variant of the Isaichev relationship described above, are summarized in Figure 8. It can be seen that the habit plane of

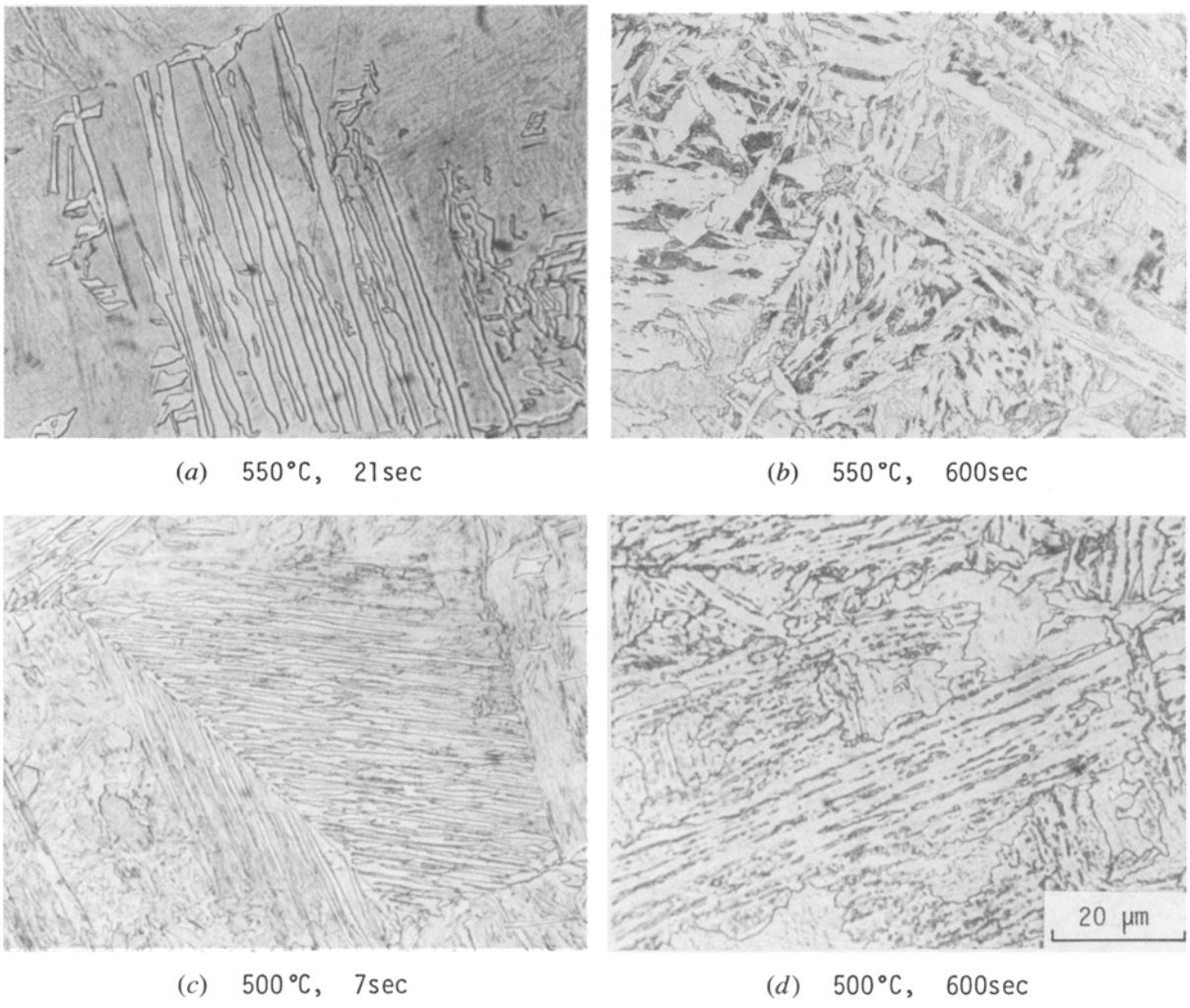

Fig. 2—Bainitic ferrite of 0.23C-0.25Si-1.86Mn steel austenitized at 1200 °C and isothermally transformed.

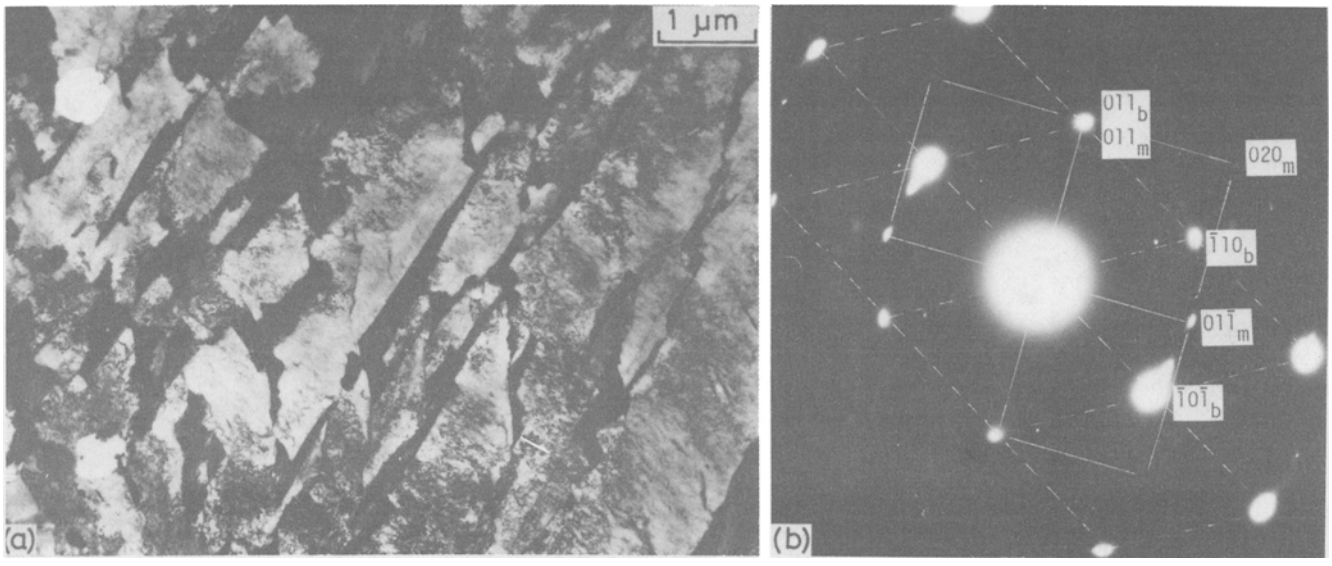

Fig. 3—Bainite laths consisting of small subunits formed by the isothermal transformation at 500 °C for 120 s of 0.20C-0.30Si-0.97Mn-1.37Cr-0.59Mo-0.0010B steel: (*a*) bright-field image and (*b*) selected area electron diffraction pattern.

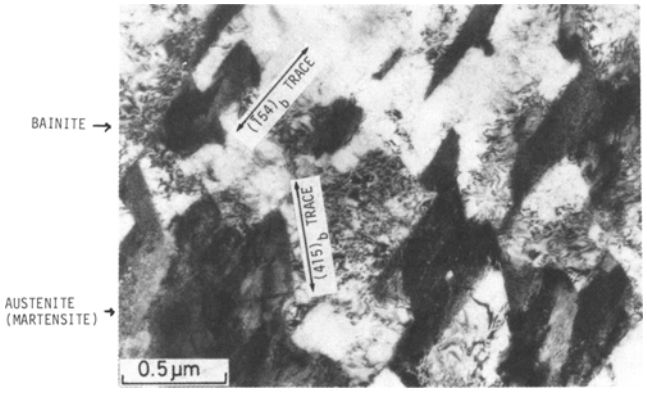

Fig. 4—Detailed structure of a subunit observed in Fig. 3.

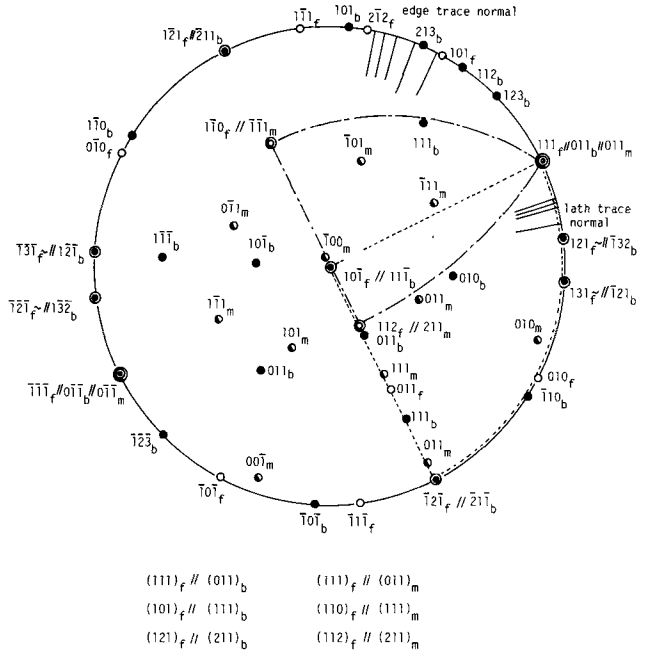

Fig. 5—The stereographic analysis of Fig. 3.

the laths lies midway between the $(111)_f$ and the $(252)_f$ planes and that the cementite platelets exhibit the habit in the vicinity of the $(415)_b \sim // (301)_c$, the latter being almost parallel to the trace normals for the edges of the bainite laths.

B. *Continuously Cooled Transformation*

Continuously cooled transformations such as quenching, normalizing, direct quenching, and accelerated cooling are apt to produce mixed structures. A nomenclature of those microstructures has been proposed.[24] However, the details of those structures are essentially the same as those of isothermal transformation products.

Figure 9 shows a CCT diagram of Ni-Cr-Mo steel. Martensite, martensite and bainite, and bainite with martensite-austenite constituents were obtained depending on cooling rate. In the vicinity of upper critical cooling rate, BIII-type bainite/martensite duplex structure was obtained.

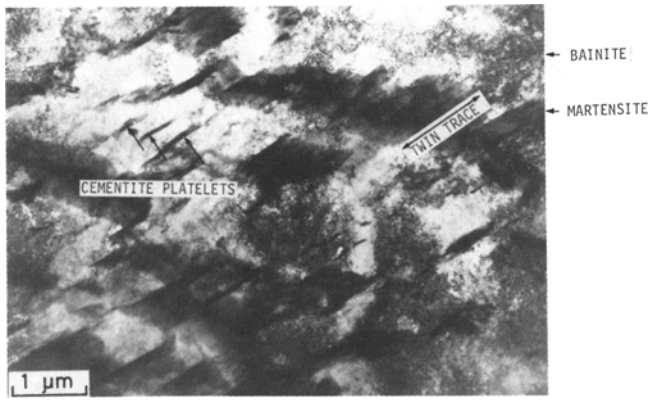

Fig. 6—The cementite platelets formed at the subunit/austenite (martensite) interphase boundaries. Isothermal transformation of 0.20C-0.30Si-0.97Mn-1.37Cr-0.59Mo-0.0010B steel at 475 °C for 60 s.

Figures 10 and 11 show CCT diagrams after hot deformation for Si-Nb-V and ultralow C-Nb-Ti-B[25] steels. In the case of the Si-Nb-V steel, the primary ferrite transformation occurs at a much higher cooling rate. Hot working makes the microstructure finer, and the austenite grain boundaries were not clearly identified due to the primary ferrite formation. In the latter case, the bainite transformation occurs without primary ferrite at a higher cooling rate, and the deformed austenite grain boundary can be seen clearly. This is one of the characteristics of the bainite transformation without primary ferrite formation.

Figure 12 shows the initial stage of bainite-lath formation of the ultralow-carbon steel cooled rapidly from 1200 °C. The mode of bainite lath observed at higher magnification is quite the same morphology as that of the 0.2C-Si-Mn steel.

Figure 13 shows the *Bs* and *Ms* temperatures measured in commercial-grade high-tensile-strength steels. The *Bs* temperatures which were measured in the regions without ferrite transformation are plotted, because *Bs* temperature goes down when ferrite transformation occurs. The relationship between *Ms* temperature and carbon content is consistent with the results by Pickering.[16] The carbon content dependency of *Bs* is much smaller than that of *Ms*. Even though carbon level is very low, *Bs* temperature increases slightly. This is probably due to the effect of the carbon partitioning that occurred at bainite nucleation. The addition of alloying elements is also attributed to the decrease of the *Bs* temperature.

IV. MECHANICAL PROPERTIES

A. *Heat-Treated Materials*

The Charpy impact properties were examined in relation to cooling. The brittle-ductile transition temperature (FATT) does not change monotonically with cooling rate, but there was an optimum cooling rate.[17] This cooling rate was confirmed to be a lower cooling rate than the critical cooling of bainite transformation, the microstructure being martensite/bainite duplex structure. This relationship was confirmed to exist in both as-continuously cooled and tempered specimens. The FATT

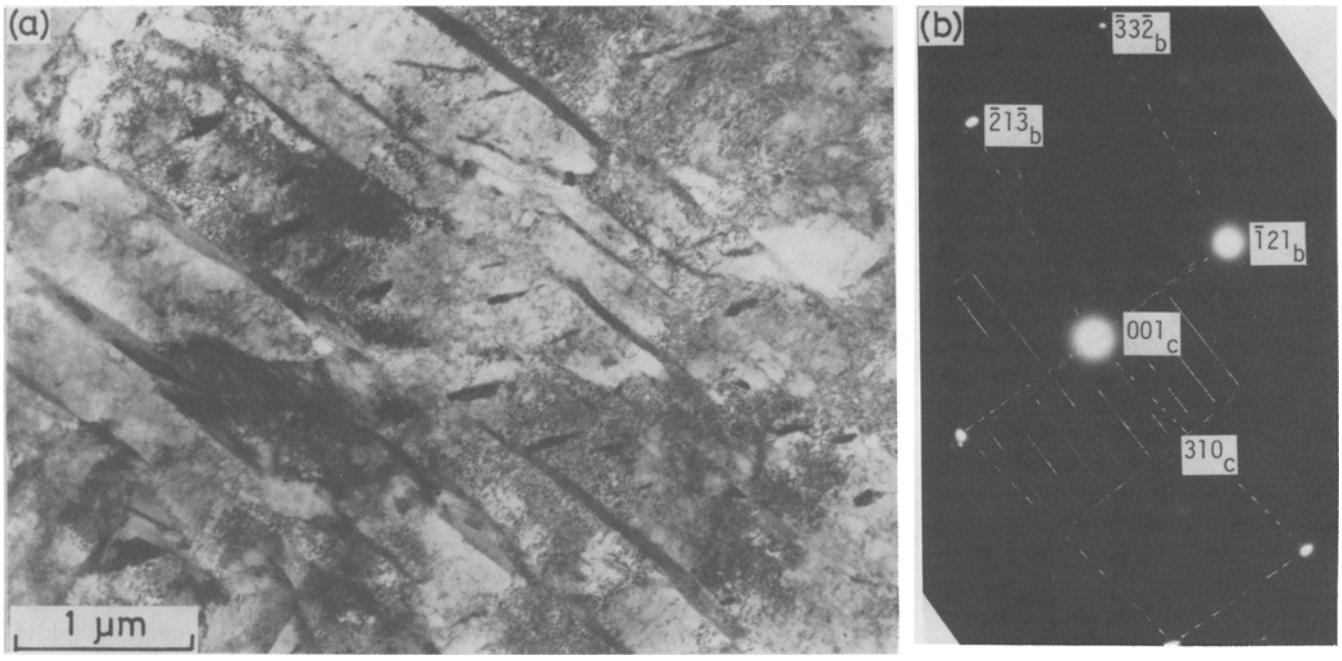

Fig. 7—Typical BIII type upper bainite formed by the coalescence of the bainite subunits. 0.20C-0.30Si-0.97Mn-1.37Cr-0.59Mo-0.0010B steel isothermally transformed at 450 °C for 120 s. Cementite platelets can be seen within the lath-like ferrite grains: (*a*) bright-field image and (*b*) selected area electron diffraction pattern.

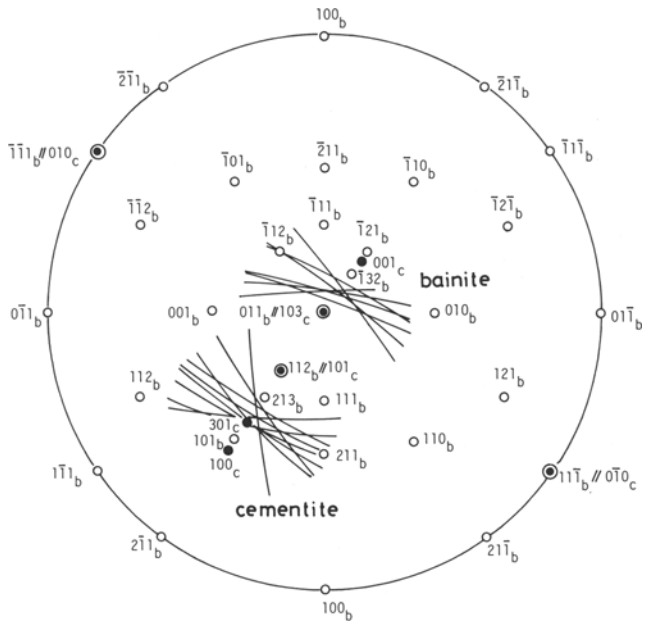

Fig. 8—Trace analysis for bainite laths and the cementite platelets within the laths by fixing the cementite/ferrite orientation relationship.

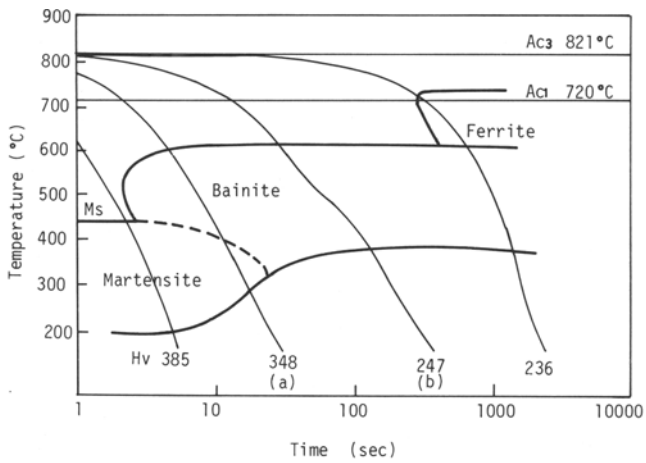

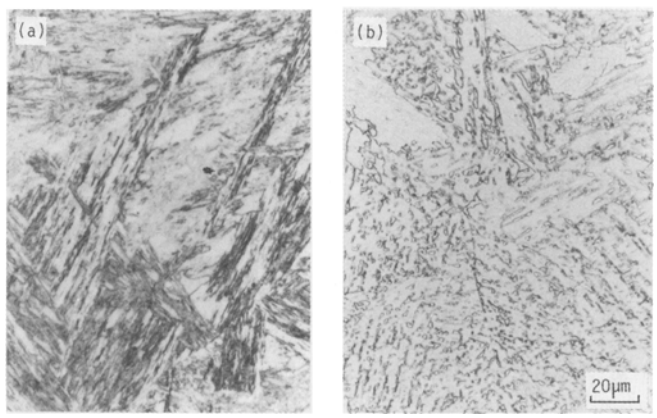

Fig. 9—CCT diagram and microstructures of 0.12C-0.30Si-0.83Mn-0.30Cu-1.11Ni-0.53Cr-0.49Mo-0.03V steel austenitized at 1200 °C and continuously cooled. Cooling rates are (*a*) 23 °C/s and (*b*) 3 °C/s.

of the BIII bainite is almost the same as that of the duplex structure. Based on the results of fracture surface examination, "the region consisting of brittle fracture planes of which orientation differences are within 10° from $(100)_b$ planes" was defined as a unit crack path.[26] Within this unit, a crack nucleates, propagates, and is arrested. It was experimentally confirmed that these units were well correlated to the Charpy impact transition temperatures. In the martensite/bainite duplex and the bainite structures, the unit crack paths were largely reduced.

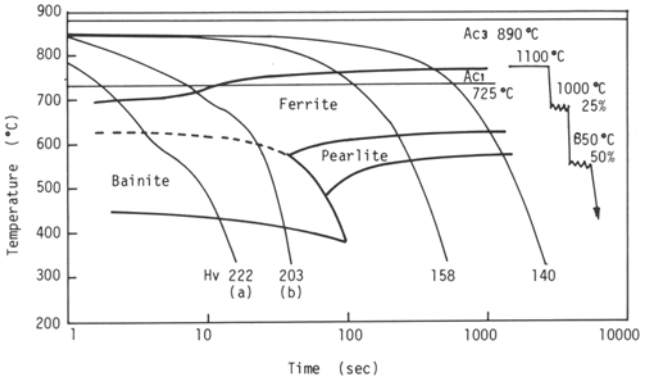

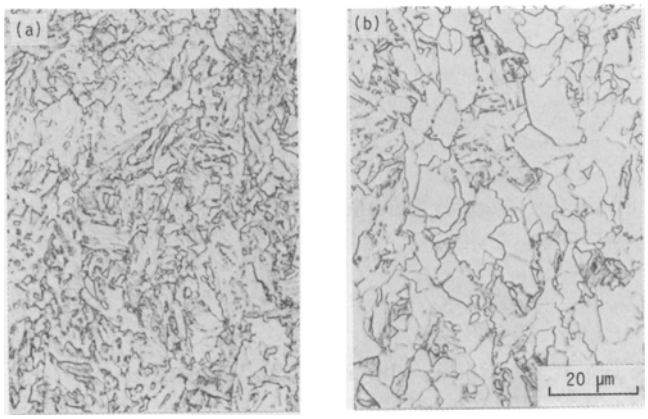

Fig. 10—Bainitic structures of 0.08C-0.28Si-1.57Mn-0.034Nb-0.07V-0.018Ti steel continuously cooled after hot deformation in austenite.

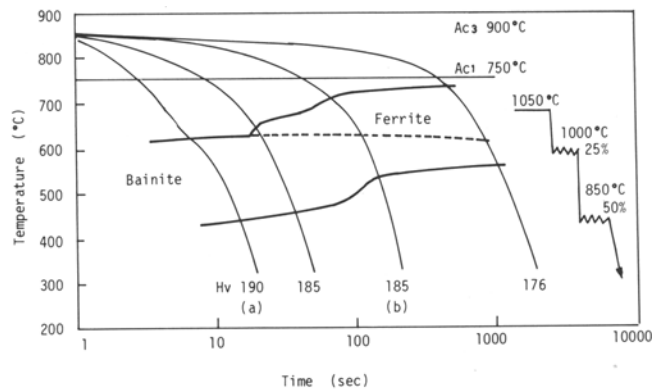

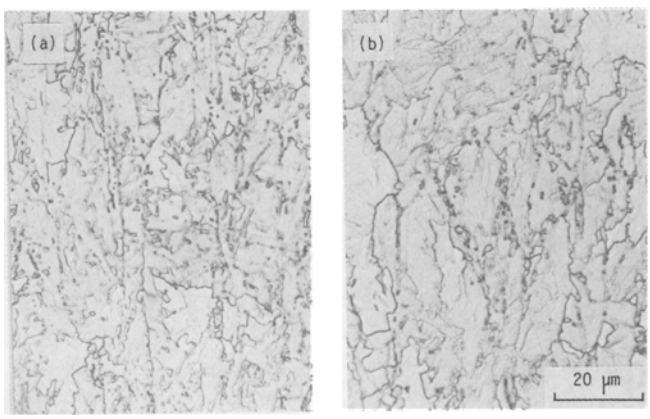

Fig. 11—Bainitic structures of 0.02C-0.16Si-1.60Mn-0.017Ti-0.043Nb-0.0018B-0.0020N steel continuously cooled after hot deformation in austenite.

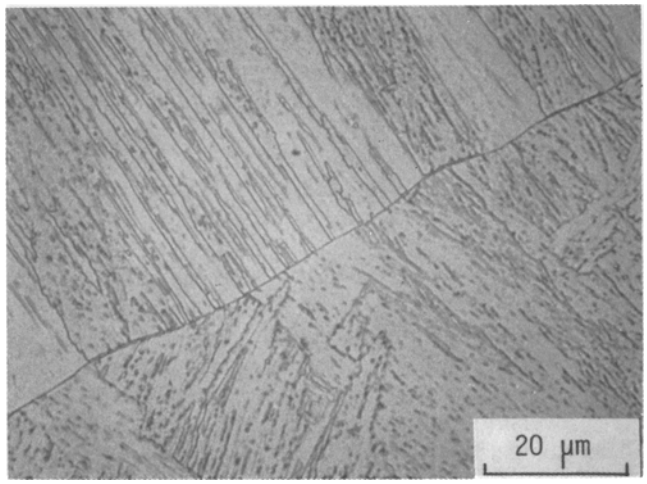

Fig. 12—Bainitic ferrite of ultralow-carbon steel. 0.03C-0.37Si-1.7Mn-0.0010B-0.02Ti-0.04Nb-0.0020N steel austenitized at 1200 °C and isothermally transformed at 630 °C for 10 s.

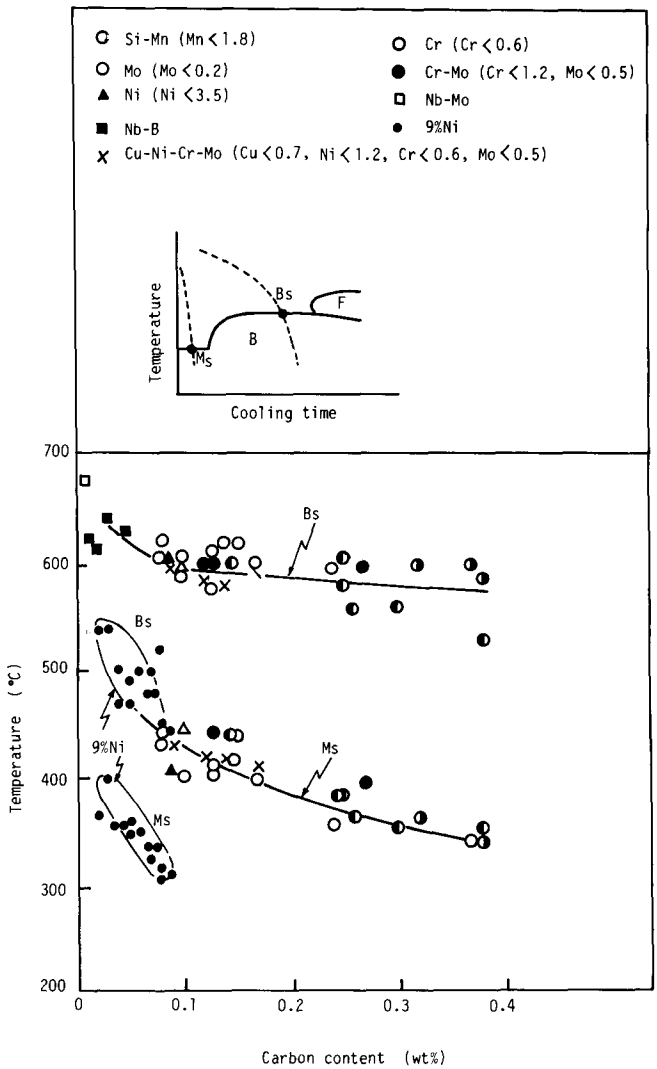

Fig. 13—*Bs* and *Ms* temperatures of commercial grade high-strength low-alloy steels measured by CCT.

These results suggest that the role of bainite in the duplex was the partitioning of an austenite grain into several parts prior to the martensite transformation,[17] the effective grain size for fracture being much finer. Figure 14 shows the variation of Charpy impact transition temperature of the bainite, of bainite/martensite duplex, and martensite structures with tempering temperature.[18] The bainite/martensite duplex and the bainite structure exhibit much better toughness than the martensite. The 500 °F (300 °C) temper embrittlement observed in the martensite is due to the cementite precipitation along the austenite grain boundary and the redistribution of impurities.[27] The materials used for this experiment have low P content and Mo addition. Therefore, reversible temper embrittlement could not be seen in the tempering range of 450 °C to 600 °C in a short-time tempering. The degradation of impact properties of martensite at 550 °C to 600 °C is thought to be due to alloy carbide precipitation such as VC and Mo_2C. Figure 15 shows the variation of strength of these structures with tempering. The strength of martensite decreases gradually at the tempering temperatures higher than 200 °C. The bainite/martensite duplex structure also has similar behavior, but it is interesting to note that the duplex structure exhibits less strength drop than the martensite structure, and the bainitic structure has little strength change below 500 °C. This is probably due to the cementite precipitation mode; *i.e.*, bainite transforms at higher temperature with cementite precipitation compared with martensite. This strength change with tempering at 200 °C to 500 °C, where the duplex structure has higher strength than the martensite, was more clearly seen in higher carbon steel.[28]

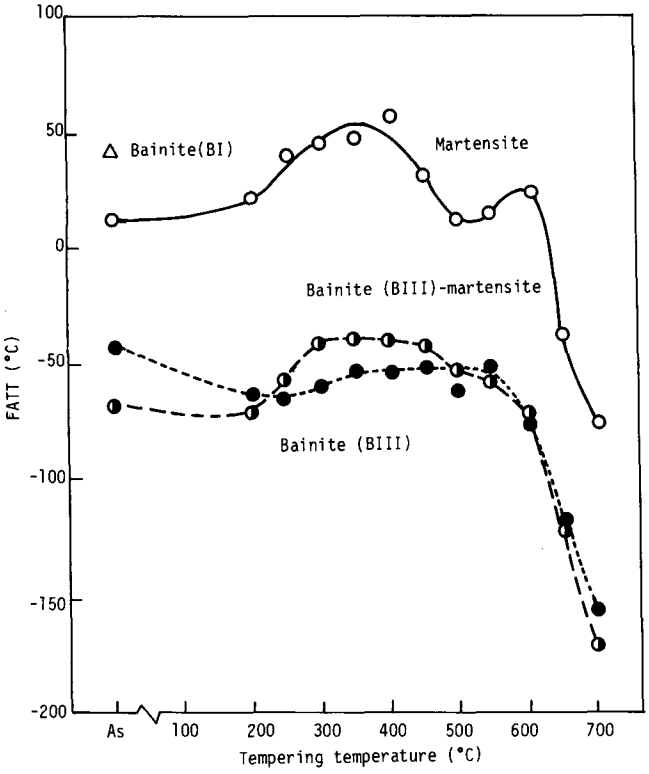

Fig. 14—Variation Charpy impact properties of martensite, bainite-martensite, and bainite with tempering temperature of 0.12C-0.30Si-0.83Mn-0.3Cu-1.11Ni-0.53Cr-0.49Mo-0.03V steel.

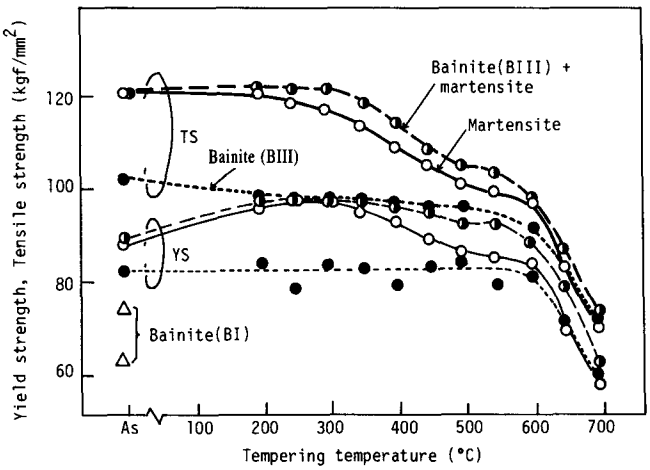

Fig. 15—Variation of tensile properties of martensite, bainite-martensite, and bainite with tempering temperature of 0.12C-0.30Si-0.83Mn-0.3Cu-1.11Ni-0.53Cr-0.49Mo-0.03V steel.

B. *Mechanical Properties of Thermomechanically Treated Structures*

Figure 16 shows the mechanical properties of the control-rolled and accelerated-cooled Nb-V steel. With lowering the cooling stop temperature, the tensile strength increased, but yield strength exhibited a minimum value at about 250 °C. This minimum probably arose from the formation of martensite or bainite islands within the soft ferrite grains. On the other hand, the FATT does not show significant change. This is due to the fact that the unit crack path does not change. The microstructure in accelerated cooling has the mixture of ferrite, bainite, and martensite, as shown in Figures 17 and 18. The volume fractions of bainite and martensite depend on the cooling stop temperature. The bainite mainly consists of BI type, and small amounts of BII and BIII can be seen. In the heat-treated case, BI bainite reduces toughness. In the accelerated specimens, however, the austenite grain is greatly refined by thermomechanical rolling, and a very fine unit crack path can be obtained.

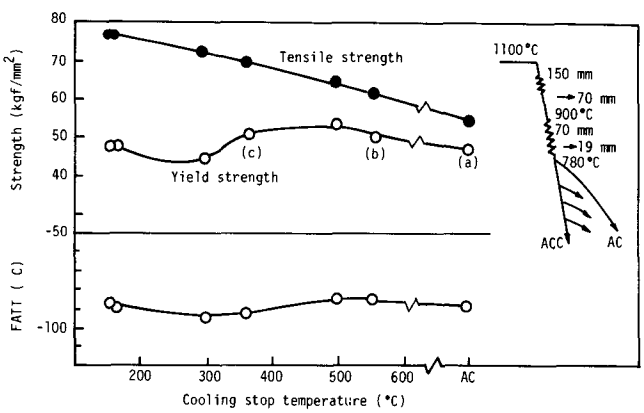

Fig. 16—Mechanical properties of accelerated-cooled 0.08C-0.28Si-1.57Mn-0.07V-0.03Nb-0.018Ti steel. Cooling rate is 15 °C to 30 °C/s. Microstructures of (a), (b), and (c) are shown in Fig. 17.

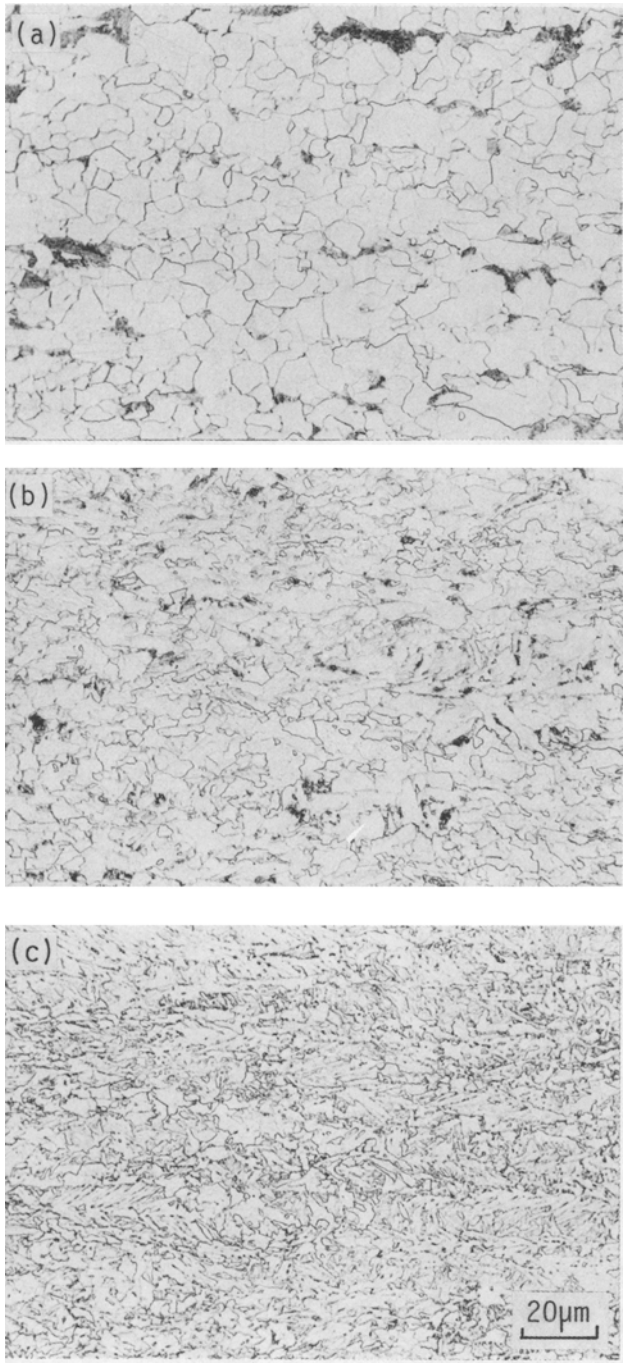

Fig. 17—Microstructures of controlled-rolled and accelerated-cooled 0.08C-0.28Si-1.57Mn-0.034Nb-0.07V-0.018Ti steel. (*a*) As-rolled and (*b*) and (*c*) accelerated cooling with cooling stop temperature at 550 °C and 360 °C, respectively.

Even in an ultralow-carbon steel, high strength can be obtained when the microstructure consists mainly of bainite, as shown in Figure 19. In this case, boron increases hardenability in conjunction with alloying elements such as Mn, Mo, Nb, and low N. The strength of air cooling and accelerated cooling is the same, but the toughness decreases in accelerated cooling. In air cooling, the prior austenite grain boundaries were decorated by a small amount of ferrite grains, but in accelerated cooling, ferrite formation did not occur and

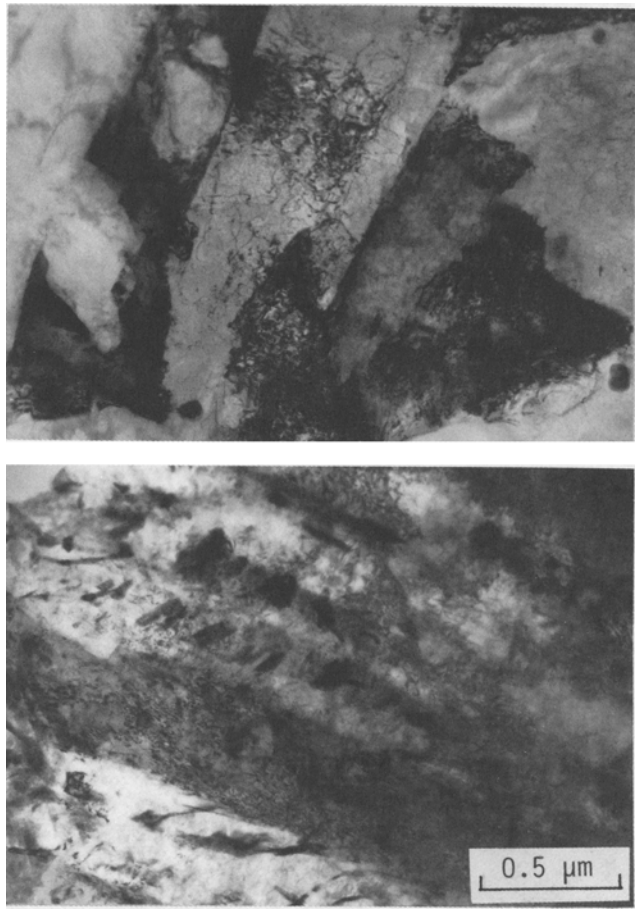

Fig. 18—Ferrite and bainite of accelerated-cooled 0.08C-0.28Si-1.57Mn-0.034Nb-0.07V-0.018Ti steel. Cooling stop temperature at 360 °C.

deformed austenite grain boundaries can be seen clearly. Therefore, ferrite formation plays an important role for toughness in this type of steel by making the unit crack path finer.[25]

V. DISCUSSION

A. *Mechanism of Bainite Transformation*

In the present study, it was confirmed that a bainitic ferrite lath consists of much finer subunits and the coalescence of them yields the lathlike upper bainite, as anticipated for low-carbon lath martensite.[20] These bainitic ferrite subunits are in the shape of the needles elongated in the $[\bar{1}01]_f \sim // [\bar{1}\bar{1}1]_b$ direction and enclosed by rather sharp edges of the $(232)_f \sim // (\bar{1}54)_b$ and the $(3\bar{1}3)_f \sim // (415)_b$ planes.

At the high temperature just below *Bs*, the diffusion of carbon in both bainitic ferrite and austenite is very rapid. Therefore, carbon diffuses to untransformed austenite without cementite precipitation (Type I bainite). This carbon-enriched austenite will transform diffusionally to pearlite when carbon is in eutectic concentration. It will decompose into low-temperature transformation products such as Type II or III bainite and martensite on rapid cooling.

In Type II and III bainite, cementite particles form as

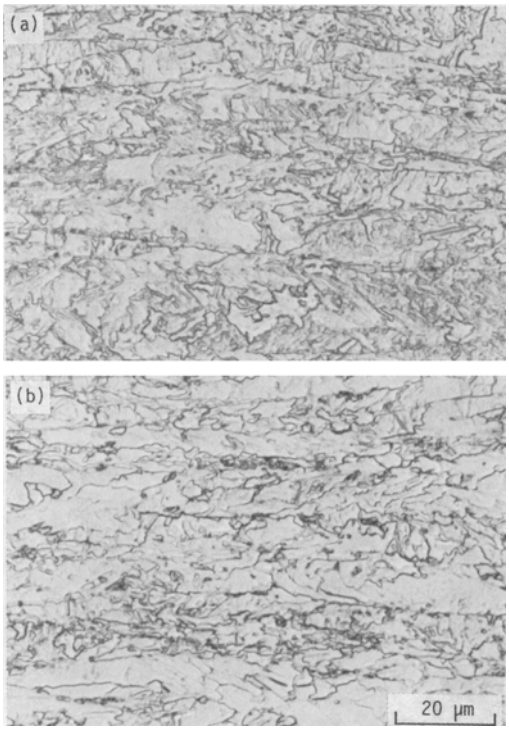

Steel	Y. S. kgf/mm^2	T. S. kgf/mm^2	E. l. %	FATT C
(a) As rolled	49.0	61.8	24.0	-92
(b) Accelerated cooling	39.5	62.0	20.8	-40

Fig. 19—Mechanical properties and microstructures of controlled-rolled and accelerated-cooled 0.02C-0.16Si-1.85Mn-0.05Nb-0.019Ti-0.0011B-0.0035N steel.

the layers between the laths as well as the fine platelets aligning parallel to a specific ferrite plane in the interior. The present study suggests that the latter configuration arises from the precipitation of cementite on the $\sim(3\bar{1}3)_f\sim//(415)_b$ subunit edges which are the sidewise growth fronts. The coalescence of the subunits produces the structure where cementite platelets appear to precipitate within the ferrite laths.[3] Such a situation can easily be imagined in the case of relatively low temperature transformation, where the rate of carbon diffusion in the austenite is slightly slower than that of the bainite growth because of carbon atom buildup.

In Type II bainite, cementite particles precipitate at the final stage of transformation after the subunit coalescence and form the layers between the ferrite laths where carbon atoms are sufficiently enriched, *i.e.*, on the $\sim(232)_f\sim//(1\bar{5}4)_b$ planes, leading to a typical so-called "upper bainite morphology." In both cases, cementite particles are thought to form at the austenite/ferrite interfaces in contact with both phases, because they exhibit a specific variant of the Isaichev orientation relationship with the ferrite instead of the Bagaryatskii relationship.[29] This orientation relationship gives an extremely good fit on the $(101)_c//(112)_b$ planes as far as iron atoms are concerned.[30] If the ferrite is related to the parent austenite by the Kurdjumov-Sachs relationship,[21] the cementite/austenite orientation relationship is much closer to that of Pitsch:[31]

$$(010)_c//(\bar{1}01)_f$$
$$(100)_c//(\bar{5}45)_f$$

in the Isaichev relationship than in the case of Bagaryatskii, implying that the cementite particles form at the austenite/ferrite interphase boundaries in contact with both phases.[22,23] This process of upper bainite formation is depicted in Figure 20. The cementite platelets precipitate at the subunit interfaces as in Figure 20(a), and the coalescence of the subunits yields the upper bainite where cementite particles form in the interior (Figure 20(b)).

It is also interesting to note that the traces of transformation twins in the martensite formed by the decomposition of the untransformed austenite are almost parallel to the sidewise growth edges of the bainite subunits. This suggests that the side edge of the bainite subunits may be parallel to the lattice invariant shear planes in the bainite transformation.

B. *Brittle-Ductile Transition Temperature*

It has been generally understood that the brittle-ductile transition temperature (FATT) depends on the ferrite grain

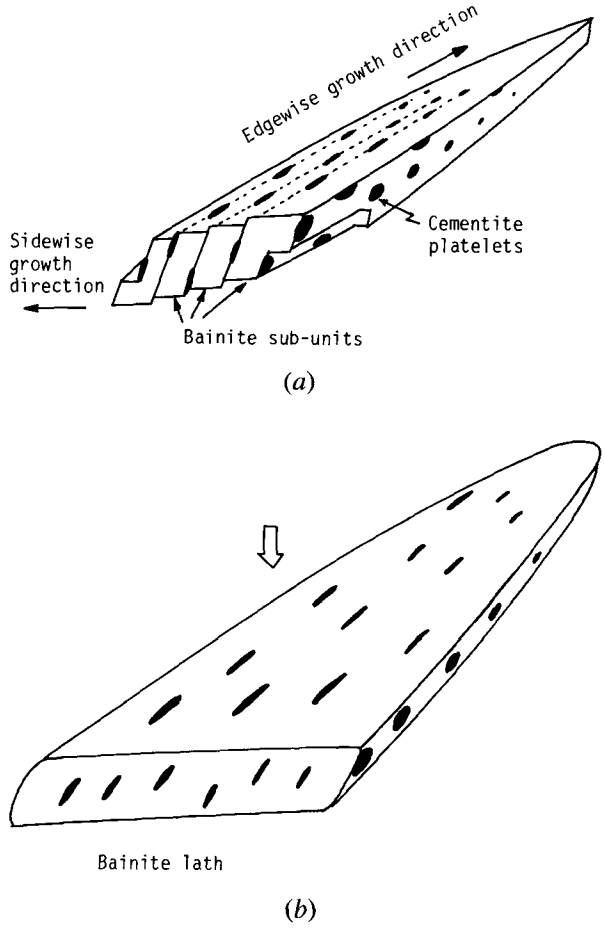

Fig. 20—Schematic illustration of BIII-type bainite formation: (*a*) cementite platelet nucleation and (*b*) coalescence of subunits.

size. It is often noted that the central portion of quenched thick plate has better toughness than the surface portion, even though the central region is cooled slower than the surface. This can be explained by the fact that BIII-type bainite or BIII bainite/martensite duplex has better toughness than martensite. The relation between the austenite grain size and the unit crack path is shown in Figure 21. At a certain austenite grain size, BIII-type bainite or duplex structure has a smaller unit crack path than martensite. When carbon level is relatively high, say 0.1 pct, BI bainite transformed in heat treatment deteriorates the toughness, because its unit crack path is large and carbon-enriched austenite between them transforms to high-carbon martensite or austenite-martensite constituents. To improve the impact properties of Type I or Type II bainite, the austenite grain size has to be refined and the carbon content lowered. In the case of accelerated cooling after controlled rolling, the austenite grain size can be much reduced, and a good toughness can be obtained without loss of strength. With controlled rolling at relatively low temperature austenite regions, the unrecrystallized elongated austenite grain remains. The BI-type bainite transformed from such elongated austenite grains has fairly large unit crack paths. In this case, strength can be obtained, but FATT cannot be improved.[25]

VI. CONCLUSIONS

The bainite transformations of low-carbon high-strength commercial steel in both isothermal holding and continuous cooling were studied. The mechanical properties of bainite-containing structures were examined.

1. At the initial stage of transformation, upper bainitic ferrite forms as the subunits elongated in the $[\bar{1}01]_f//[\bar{1}\bar{1}1]_b$ and enclosed by the surfaces comprising the $(232)_f\sim//(\bar{1}54)_b$ and the $(3\bar{1}3)_f\sim//415)_b$ planes.
2. Coalescence of the subunits yields the lathlike upper bainite with the $[\bar{1}01]_f$ $(232)_f$ habit.
3. Based on the appearance of cementite, the upper bainite is classified into three types: Type I is carbide-free ferrite; Type II is typical upper bainite with cementite precipitation between laths; and Type III has cementite platelets aligned in the interior of bainitic ferrite laths.
4. Cementite particles precipitate on the sidewise growth tips of the bainitic ferrite subunits, *i.e.*, on the $(3\bar{1}3)_f\sim//(415)_b$. This results in the cementite platelets aligned parallel to a specific ferrite plane in the laths after the coalescence.
5. This morphology of bainite is essentially the same in lower carbon high-strength steels.
6. In the specimens accelerated cooled after controlled rolling, the microstructure generally comprises mixtures of various types of transformation structures.
7. In the quenched and tempered specimens, BIII bainite and BIII bainite/martensite duplex structure have better toughness than martensite. This is explained by fine unit crack paths.
8. Bainite has less strength change than martensite on tempering, and it does not exhibit the 500 °F temper embrittlement.
9. BIII bainite/martensite duplex structure has higher strength than martensite in tempering between 200 °C and 500 °C.
10. To improve the toughness of thermomechanically treated specimens, austenite grain refinement and a small amount of ferrite formation prior to bainite transformation are important.

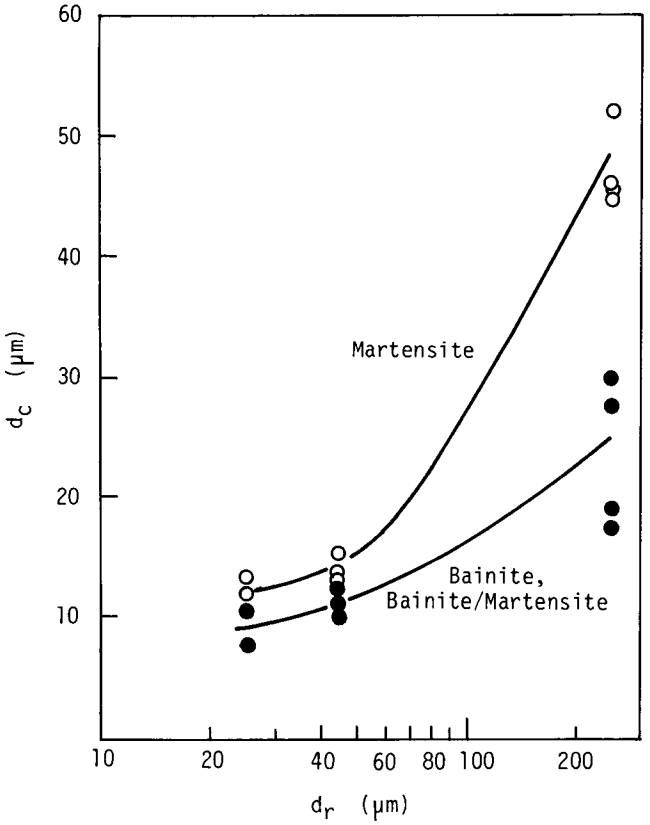

Fig. 21—Relation between austenite grain size (d_r) and unit crack path (d_c) in 0.12C-0.30Si-0.83Mn-0.3Cu-1.11Ni-0.53Cr-0.49Mo-0.03V steel.

REFERENCES

1. A.B. Greninger and A.R. Troiano: *Trans. TMS-AIME*, 1940, vol. 140, pp. 307-36.
2. W. Hume-Rothery: *The Structures of Alloys of Iron*, 1966, Pergamon Press, London, p. 246.
3. Y. Ohmori, H. Ohtani, and T. Kunitake: *Trans. Iron Steel Inst. Jpn.*, 1971, vol. 11, pp. 250-59.
4. R.W.K. Honeycombe and F.B. Pickering: *Metall. Trans.*, 1972, vol. 3, pp. 1099-1112.
5. N.F. Kennon: *Metall. Trans. A*, 1978, vol. 9A, pp. 57-66.
6. A.T. Davenport: *Proc. Int. Conf. Solid-Solid Phase Transformations*, Pittsburgh, PA, 1981; as referred to by M. Srikaya and G. Thomas: *J. Phys. Colloq.*, 1982, Supp. 12, Tome 43, pp. C4, 563-68.
7. S.J. Matas and R.F. Heheman: *Trans. TMS-AIME*, 1961, vol. 221, pp. 179-85.
8. R.I. Entin: in *Decomposition of Austenite by Diffusional Processes*, H.I. Aaronson, ed., 1962, pp. 295-311.
9. J.M. Oblak and R.F. Heheman: *Transformation and Hardenability in Steels*, Climax Molybdenum Company, Ann Arbor, MI, 1967, pp. 15-29.
10. R. Le Houillier, C. Bégin, and A. Dubé: *Metall. Trans.*, 1971, vol. 2, pp. 2645-53.
11. E.P. Simonen, H.I. Aaronson, and R. Trivedi: *Metall. Trans.*, 1973, vol. 4, pp. 1239-45.

12. H.K.D.H. Bhadeshia and D.V. Edmonds: *Metall. Trans. A*, 1979, vol. 10A, pp. 895-907.
13. H.K.D.H. Bhadeshia and D.V. Edmonds: *Met. Sci.*, 1983, vol. 17, pp. 411-19.
14. G. Papadimitriou and J.M. Génin: *Abstr. of Int. Conf. Martensitic Transformations (ICOMAT-86)*, Japan Institute of Metals, 1986, pp. 607-12.
15. K. Shimizu, T. Ko, and Z. Nishiyama: *Trans. Jpn. Inst. Met.*, 1964, vol. 221, pp. 225-30.
16. F.B. Pickering: *Transformation and Hardenability in Steels*, Climax Molybdenum Company, Ann Arbor, MI, 1967, pp. 109-29.
17. H. Ohtani, F. Terasaki, and T. Kunitake: *Trans. Iron Steel Inst. Jpn.*, 1972, vol. 12, pp. 118-27.
18. Y. Ohmori, H. Ohtani, and T. Kunitake: *Met. Sci.*, 1974, vol. 8, pp. 357-66.
19. Y. Ohmori, H. Ohtani, and T. Kunitake: *Trans. Iron Steel Inst. Jpn.*, 1972, vol. 12, pp. 146-54.
20. Y. Ohmori: *Phil. Mag. A*, 1988, vol. 57, pp. 337-49.
21. G.V. Kurdjumov and G. Sachs: *Zeit. Phys.*, 1930, vol. 64, pp. 325-43.
22. Y. Ohmori: *Trans. Iron Steel Inst. Jpn.*, 1973, vol. 13, pp. 56-62.
23. Der-Hung Huang and Gareth Thomas: *Metall. Trans. A*, 1977, vol. 8A, pp. 1661-74.
24. B.L. Bramfitt and J.G. Speer: *Metall. Trans. A*, 1990, vol. 21A, pp. 817-29.
25. Y. Fujishiro, T. Hashimoto, and H. Ohtani: *Tetsu-to-Hagané*, 1989, vol. 75, pp. 143-50.
26. F. Terasaki and H. Ohtani: *Trans. Iron Steel Inst. Jpn.*, 1972, vol. 12, pp. 45-53.
27. J.R. Rellick and C.J. McMahon, Jr.: *Metall. Trans.*, 1974, vol. 5, pp. 2439-50.
28. T. Tsumura and H. Ohtani: *J. Jpn. Soc. Heat-Treat.*, 1988, vol. 28, pp. 213-19.
29. A. Bagaryatskii: *Dokl. Akad. Nauk SSSR*, 1950, vol. 73, p. 1161; referred to by K.W. Andrews: *Acta Metall.*, 1950, vol. 11, pp. 939-46.
30. Y. Ohmori, A.T. Davenport, and R.W.K. Honeycombe: *Trans. Iron Steel Inst. Jpn.*, 1972, vol. 12, pp. 128-37.
31. W. Pitsch: *Arch. Eisenhuettenwes.*, 1963, vol. 34, pp. 641-45.